Tumor Biol. (2016) 37:10643–10652
DOI 10.1007/s13277-016-4961-x

ORIGINAL ARTICLE

iRGD-targeted delivery of a pro-apoptotic peptide activated by cathepsin B inhibits tumor growth and metastasis in mice

Wang Qifan[1] · **Ning Fen**[2] · **Xue Ying**[1] · **Feng Xinwei**[1] · **Du Jun**[1] · **Zhang Ge**[1]

Received: 5 November 2015 / Accepted: 2 February 2016 / Published online: 11 February 2016

Abstract The use of cytolytic peptides with potential therapeutic properties is a promising approach to cancer therapy due to their convenient automated synthesis and their capacity for modifications. However, the use of cytolytic peptides is limited due to their nonspecific cytolytic activity. In this study, we designed a tumor-targeting proapoptotic system based on an amphipathic D-amino acid-modified apoptotic peptide, KLA, a variant of $(KLAKLAK)_2$, which is fused with a linear tumor-penetrating homing peptide iRGD through specific cathepsin B (CTSB) cleavage sequences that are overexpressed in many types of tumor tissues. Our data show that the procytotoxic peptide $_D$(KLAKLAKKLAKLA)K-GG-iRGD (m(KLA)-iRGD) is internalized into cultured tumor cells through a neuropilin-1 (NRP1)-activated pathway by iRGD delivery. Once inside the cells, the peptide triggers rapid apoptosis through both the mitochondrial-induced apoptotic pathway and the death receptor pathway in NRP1+/αvβ3/CTSB+ tumor cells. Furthermore, m(KLA)-iRGD spread extensively within the tumor tissue when it was injected into 4T1 tumor-bearing mice. The m(KLA)-iRGD peptide inhibited tumor growth to a certain degree, resulting in a significant reduction in tumor volume ($P<0.05$) and the total inhibition of metastasis at the end of the treatment. These results suggest that m(KLA)-iRGD has the potential for development as a new antitumor drug.

Keywords iRGD · Cathepsin B · Tumor growth · Metastasis

Introduction

Poor penetration into tumor tissue and adverse effects on normal cells limit the therapeutic efficacy of many chemotherapeutic drugs [1, 2]. Peptide-based antitumor therapeutic agents, which have high specificity and tissue penetration, provide a promising solution to these problems [3]. However, the high toxicity of many potential therapeutic peptides caused by nonspecific lytic activity causes them to be of limited use. Further improvements to increase the efficacy of anticancer drugs by rational design and modifications are required.

The polycation antimicrobial peptide KLA, $(KLAKLAK)_2$, can initiate apoptosis in mammalian cells by disrupting the mitochondrial membrane [4, 5]. Recently, the KLA peptide has been explored for its use as an anticancer peptide, either alone or in combination with other conventional drugs [6, 7]. The $_D$(KLA) peptide is composed of an amphipathic D-amino acid peptide that exhibits high resistance against protein degradation [8]. However, the KLA peptide has poor eukaryotic cell-penetrating potential and requires the assistance of other cell-penetrating peptides to translocate into tumor tissues.

Tumor-penetrating homing peptides have recently been used as drug carriers. Internalizing RGD (iRGD) with a sequence of CRGDKGPDC is a cyclic peptide that is capable of delivering drugs to extravascular tumor tissue. iRGD targets

Electronic supplementary material The online version of this article (doi:10.1007/s13277-016-4961-x) contains supplementary material, which is available to authorized users.

✉ Zhang Ge
zhangge@mail.sysu.edu.cn

[1] Department of Microbial and Biochemical Pharmacy, School of Pharmaceutical Sciences, Sun Yat-sen University, No.132 Wai huan dong Road, University Town, Guangzhou 510006, China

[2] Guangzhou Institute of Pediatrics, Department of Obstetrics, Guangzhou Women and Children's Medical Center, Guangzhou, China

tumor tissue using the RGD motif as a ligand for αvβ3, αvβ5, and α5β1 integrins, which are expressed abundantly in tumor vessels. Then, proteolytic processing of iRGD in tumors activates the cryptic CendR motif (R/KXXR/K) and binds to neuropilin-1 (NRP1), which is overexpressed in both angiogenic blood vessels and tumor cells, to carry the drug into the tumor tissue [9]. Moreover, iRGD was reported to have antimetastatic activity and to inhibit spontaneous metastasis in mice [10]. Recently, linear iRGD fused to the C-terminus of recombinant proteins was used to carry drugs into tumor tissues [4, 11, 12].

Many studies have shown that iRGD has successfully been used as a tumor vessel-targeting drug delivery system [13, 14]. However, αvβ3/5 integrins and NRP1 are also expressed in nontumor-associated cell. The expression of αvβ3 is observed in all angiogenic endothelial cells, such as cells involved in wound repair [15]. NRP1 is widely expressed in normal mature and developing vasculature. NRP1 has also been detected in normal, nonvascular tissues, including hematopoietic cells, immunocytes and neurons [16]. The addition of novel peptide designs to specifically target tumor cells would be expected to reduce drug side effects.

Cathepsin B (CTSB) is a lysosomal cysteine protease that promotes tumorigenesis, angiogenesis, invasion, and metastasis by endopeptidase activity involved in the degradation of the extracellular matrix [17]. Overexpression of CTSB has been observed in the cytoplasm of tumors and in human tumor-associated cells [18, 19]. CTSB represents a potential target in cancer because it can be designed as a CTSB-activated agent for both diagnosis and therapeutics [20].

In the present study, we conjugated $_{D}$(KLAKLAKKLAKLA) $_{L}$K, a variant of $_{D}$(KLAKLAK)$_2$, with a linear iRGD sequence via a GG bridge to produce the $_{D}$(KLAKLAK)$_2$K-iRGD peptide in which the -$_{D}$(A)K- amino acid bond is a unique subtractive of CTSB (Suppl. Fig 1 and Suppl. Fig 2). We hypothesized that the dual targeting of the m(KLA)-iRGD peptide would enhance cell internalization and the cytotoxicity of the peptide. To validate this hypothesis, we examined the tumor targeting and antitumor capabilities of the peptide in vitro and in vivo.

Results

Reduction of cell viability by $_{m}$(KLA)-iRGD peptide

The expression of CTSB, NRP1, and αvβ3 was detected by Western blotting in human breast cancer cells MDA-MB-231 and SKBR3, mouse breast cancer cells 4T1, and melanoma cells B16, respectively (Suppl. Fig 3). Integrin αvβ3 was detected in all four cell lines. In addition, higher expression levels of CTSB were detected in MDA-MB-231 cells, 4T1 cells, and B16 cells but not in SKBR3 cells. The expression level of NRP1 was detected in MDA-MB-231 cells, 4T1 cells, and SKBR3 cells but not in B16 cells.

The four indicated cell lines were treated with 0, 10, 20, 30, 40 μM m(KLA)-iRGD, $_{D}$(KLA)-iRGD, $_{D}$(KLA), and iRGD for 24, 48 (data not shown), and 72 h, and then, the inhibition rate was measured by MTT analysis. The results showed that m(KLA)-iRGD inhibited cell proliferation of MDA-MB-231 and 4T1 cells (CTSB+/NRP1+) in a dose-dependent manner at a concentration of 20 μM at 72 h ($P < 0.001$), whereas it was less cytotoxic to B16 cells (CTSB+/NRP1−) and SKBR3 cells (CTSB−/NRP1+) when the higher concentration of 40 μM was used (Fig. 1a–d). Morphological changes in the cells were observed using phase-contrast microscopy at 20 μM m(KLA)-iRGD, and significantly decreased cell number and morphological changes in MDA-MB-231 and 4T1 cells were observed (Fig. 1e). In addition, $_{D}$(KLA)-iRGD showed modest effects or no effect on the four indicated cell lines at the highest concentration of 40 μM. Furthermore, $_{D}$(KLA) and iRGD alone did not inhibit cell proliferation (Fig. 1a–d). These results indicate that m(KLA)-iRGD (but not $_{D}$(KLA)-iRGD or control peptides) inhibits CTSB+/NRP1+ solid tumor cell proliferation, and the modified L-enantiomer of lysine (K) at the N-terminus of $_{D}$(KLA) enhanced CTSB-activated cytotoxicity. Additionally, m(KLA)-iRGD had no effect on the CTSB−/NRP1− tumor cell, indicating that m(KLA)-iRGD is nontoxic to normal cells that are CTSB−/NRP1− in tissues.

Internalization of m(KLA)-iRGD peptide into cells

To determine whether the newly synthesized m(KLA)-iRGD peptide possessed tumor targeting, tumor-penetrating, and cell-internalizing capabilities, the C-terminus of m(KLA)-iRGD was labeled with 5-FITC, and the peptide's binding ability to several cancer cell lines was examined. Cells were observed under a confocal microscope after treatment with 3 μM FITC-m(KLA)-iRGD for 2 h. The results showed that FITC-m(KLA)-iRGD was bound to αvβ3 and NRP1-positive cells MDA-MB-231, SKBR3, and 4T1, whereas it did not bind to the NRP1-negative B16 cells (Fig. 2a). Moreover, FITC-m(KLA)-iRGD showed rapid cellular uptake at 1 h. In MDA-MB-231 and 4T1 cells, the amount of internalized FITC-m(KLA)-iRGD peaked at approximately 2 h and much of the fluorescence was observed in the cytoplasm (Fig. 2b). These results clearly establish the cell-internalizing capabilities of $_{m}$(KLA)-iRGD in NRP1+/αvβ3+ double positive cells.

m(KLA)-iRGD induces apoptosis through mitochondrial and Fas-dependent pathways

To identify whether $_{m}$(KLA)-iRGD reduced the cell proliferation by inducing apoptosis, we treated MDA-MB-231 and 4T1 cells with 20 μM m(KLA)-iRGD for 24, 48, and 72 h.

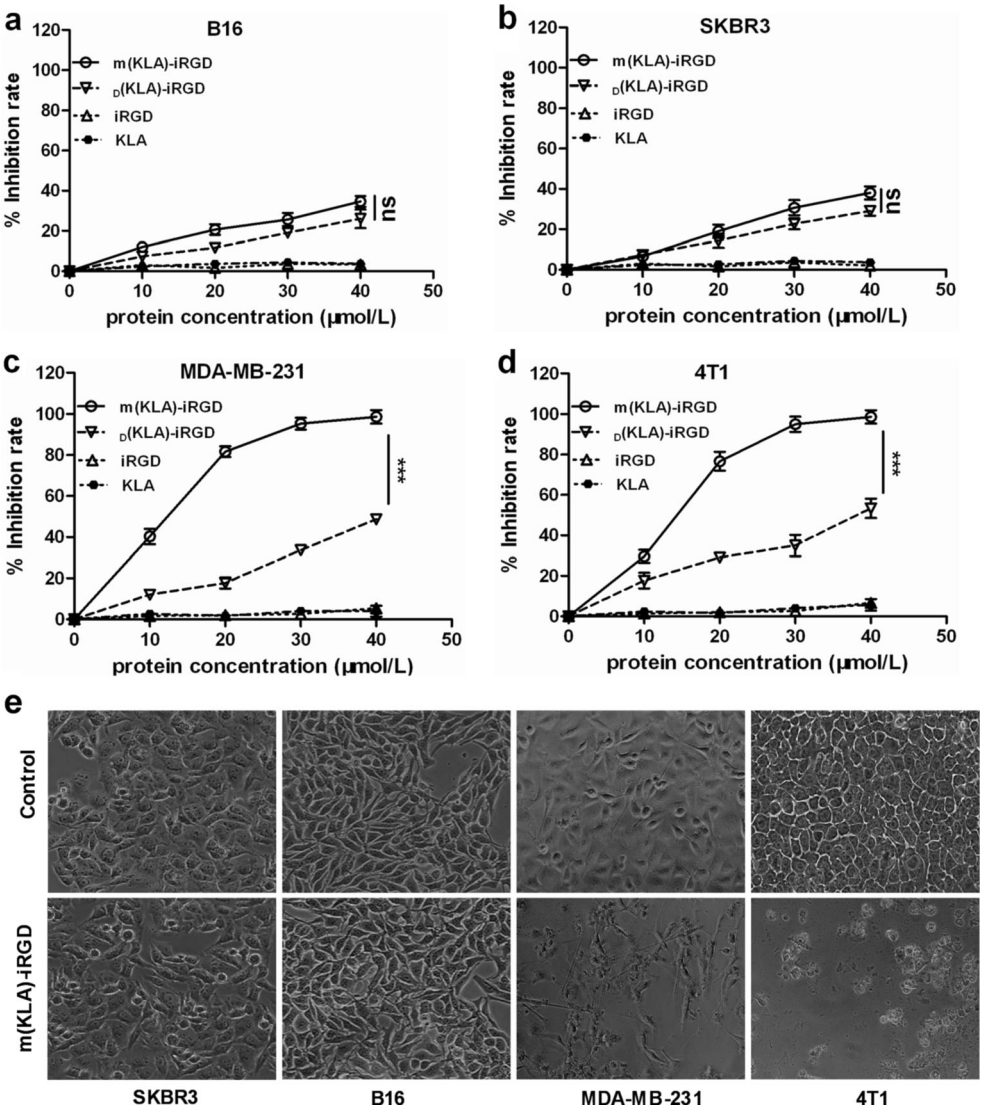

Fig. 1 Reduction of cell viability by the $_{m}$(KLA)-iRGD peptide. SKBR3 (**a**), B16 (**b**), 4T1 (**c**), and MDA-MB-231 (**d**) cells were treated with the peptides at 0, 10, 20, 30, and 40 μM for 72 h, and cell viability was measured by an MTT assay. The cellular morphology was observed following incubation for 72 h with 20 μM m(KLA)-iRGD (**e**). Representative cellular results are shown. The differences in survival rates between 20 and 40 μM m(KLA)-iRGD are more significant in both 4T1 and MDA-MB-231 cells ($P < 0.001$). However, little effect was seen on CTSB-negative SKBR3 or NRP1-negative B16 cell proliferation (ns). ***$P < 0.001$, *ns* not significant

The rates of apoptosis were determined by FACS using FITC-Annexin V and propidium iodide (PI) staining. MDA-MB-231 and 4T1 cells treated with m(KLA)-iRGD peptide showed cell shrinkage, membrane disintegration, and nuclear condensation fragmentation, which are characteristic morphological changes of cells undergoing apoptosis. However, m(KLA)-iRGD did not affect B16 and SKBR3 cell viability and morphology, as shown by phase-contrast microscopy (data not shown). FACS analysis also indicated that m(KLA)-iRGD induced cellular apoptosis in a dose-dependent manner at doses of 20 μM or higher (Fig. 3a, b). We then examined the expression of caspase-3 and Bcl-2 in the treated cells by Western blotting. Bands corresponding to full-length caspase-3 (32 kDa), cleaved caspase-3 (19 kDa), cleaved caspase-8 (18 kDa), cleaved caspase-9 (37 kDa), and Bcl-2 (26 kDa) were detected (Fig. 3c). These results indicate that m(KLA)-iRGD activates both the Fas death receptor pathway and the mitochondrial apoptotic pathway.

Penetration of m(KLA)-iRGD into tumor tissue in vivo

To confirm whether m(KLA)-iRGD could penetrate extravascular tumor tissue in vivo, FITC-m(KLA)-iRGD was injected into 4T1 tumor-bearing mice intravenously. The mice were sacrificed, and tissues were collected and imaged by an in vivo imaging system. The results showed that intravenously administered FITC-m(KLA)-iRGD peptide accumulated in the tumors after 6 h but did not accumulate in the other nontumor tissues (Fig. 4a, b). The dynamic biodistribution of FITC-conjugated m(KLA)-iRGD in tumors was analyzed at 1, 6, and 12 h using a confocal microscope. The tumor penetration activity was apparent at 1 h. The results showed that m(KLA)-iRGD was bound strongly to the tumor tissue and even penetrated several cell layers because the strong fluorescent signal was detectable in all of the sections from an entire tumor at 6 h (Fig. 4c–e) and could persist at high levels for 12 h, which indicates that the peptide is stable

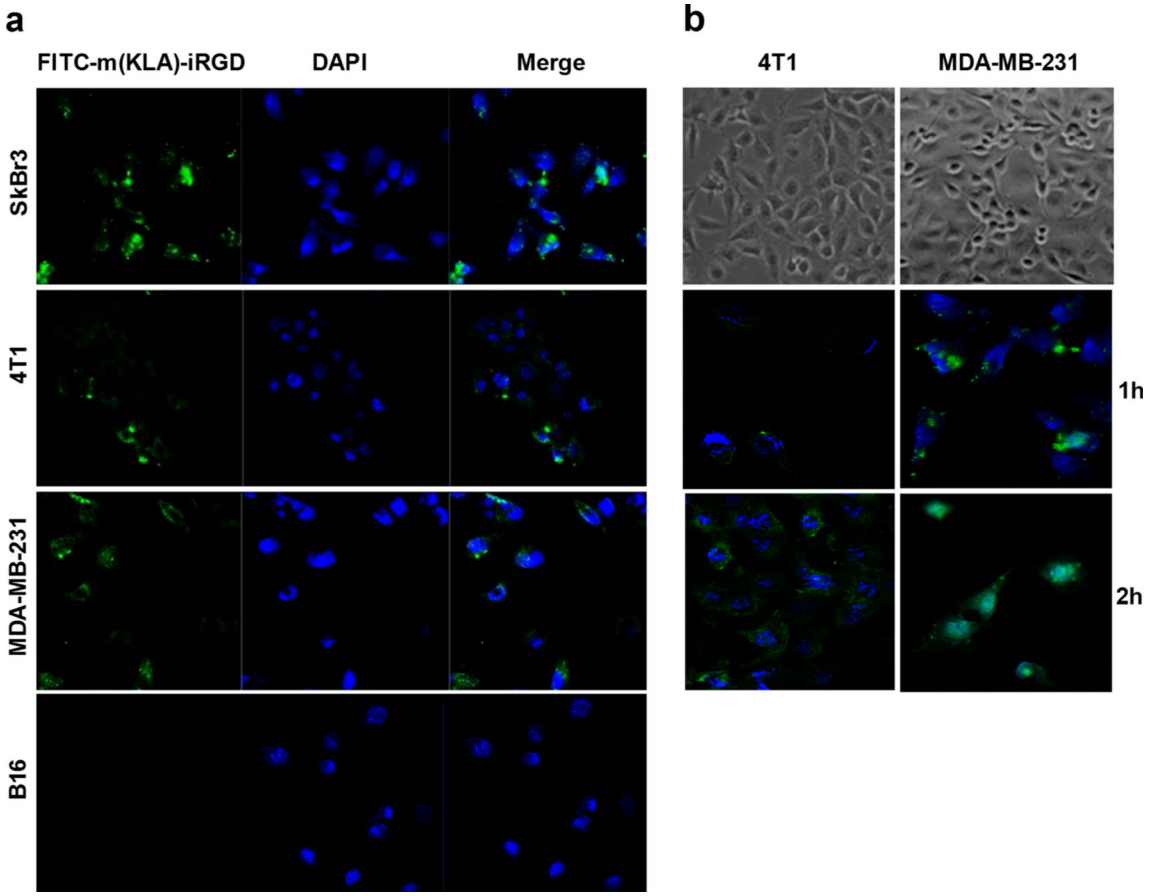

Fig. 2 Internalization of m(KLA)-iRGD peptide in cells. **a** Fluorescent images of SKBR3, 4T1, MDA-MB-231, and B16 cells treated with 3 μM FITC-m(KLA)-iRGD for 2 h as examined with confocal microscopy. Cell nuclei were stained with DAPI (*blue*). **b** Fluorescent images of MDA-MB-231 and 4T1 cells incubated with 3 μM FITC-m(KLA)-iRGD for 1 and 2 h

in vivo (Fig. 5f). Sporadic localized fluorescent signals were observed throughout the tumor, suggesting protein penetration by active transport. These data support the notion that m(KLA)-iRGD can penetrate and accumulate in tumor tissue selectively through the iRGD-mediated delivery system.

Inhibitory effect of m(KLA)-iRGD on tumor growth and tumor metastasis in vivo

To explore whether m(KLA)-iRGD peptide could represent a possible therapeutic strategy to suppress tumor growth and metastasis in vivo, the peptide's antitumor activity was evaluated in a mouse breast tumor model. 4T1 cells were injected into BALB/c mice, and m(KLA)-iRGD was administered intravenously at a dose corresponding to the mouse body weight every other day once the tumor volume reached 50 mm^3. The results showed that 4T1 tumors grew rapidly in mice treated with phosphate-buffered saline (PBS) injections, while in the m(KLA)-iRGD treated mice, inhibition of tumor growth was evident as early as 5 days after treatment began. At the end of treatment on day 21, the average tumor volume was reduced by approximately 30 % compared with the PBS control ($P = 0.011$) (Fig. 5a and Suppl. Fig 4). At the end of the experiments, the mean weight of the tumors in the m(KLA)-iRGD group was approximately 50 % lower than that in the control group, which is in agreement with the tumor size measurements ($P = 0.018$) (Fig. 5b). The mice treated with m(KLA)-iRGD did not show significant body weight loss compared to the control (data not shown).

H&E-stained tumor sections showed significant differences among tumors treated with m(KLA)-iRGD and PBS. Compared with the control, m(KLA)-iRGD-treated 4T1 mice tumor histologic sections showed significantly low tumor cell density ($P = 0.024$) (Fig. 5c). Furthermore, apoptosis of tumor cells was detected using a TUNEL assay. The number of observed apoptotic cells obviously increased in the m(KLA)-iRGD peptide-treated group relative to the control (Fig. 5d).

In addition, five of six 4T1 mice treated with PBS showed obvious lung metastasis, while none of the six m(KLA)-iRGD-treated mice showed metastasis in vivo, which indicates the inhibitory effect of the peptide on tumor metastasis in the lung or liver (Fig. 6).

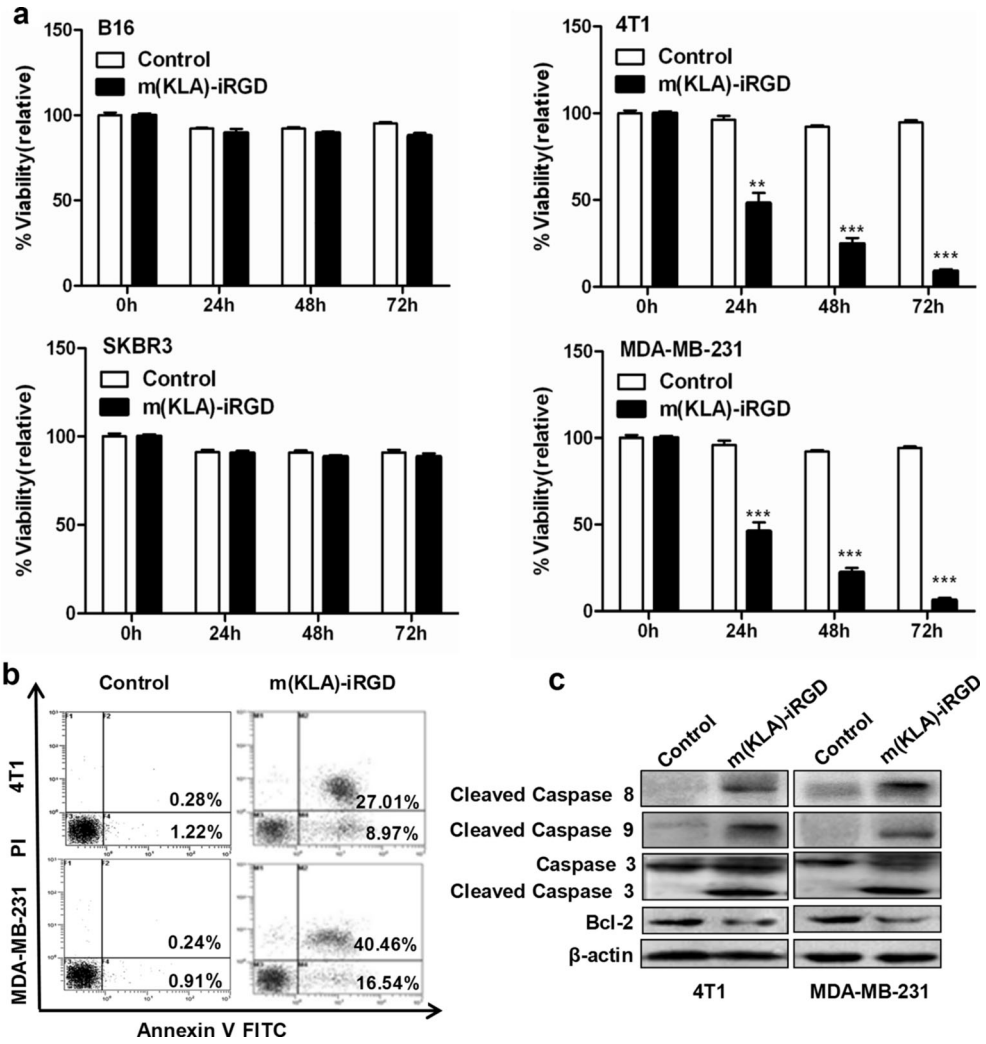

Fig. 3 m(KLA)-iRGD induces apoptosis through mitochondrial and Fas-dependent pathways. **a** Cells were treated with 20 μM m(KLA)-iRGD peptide and then analyzed by FACS for 24, 48, and 72 h. **b** The cell viability of 4T1 and MDA-MB-231 cells treated with 20 μM m(KLA)-iRGD peptide for 24 h were analyzed by flow cytometry. **c** Cultured cells treated with 20 μM m(KLA)-iRGD peptide for 24 h were harvested and lysed, and the expression of caspase-3, cleaved caspase-3, cleaved caspase-8, cleaved caspase-9, and Bcl-2 was analyzed by Western blotting. $^{**}P < 0.01$;$^{**}P < 0.001$

Collectively, these results suggest that m(KLA)-iRGD treatment significantly decreases tumor growth and metastasis in vivo.

Discussion

In this study, we synthesized the antitumor targeting proapoptotic peptide m(KLA)-iRGD and identified the potential of this approach for cancer therapy.

The KLA peptide $(KLAKLAK)_2$ is one of the most successful artificially synthesized cytolytic peptides that is inert outside of cells but becomes toxic when internalized. KLA peptides can induce considerable mitochondrial swelling at a concentration of approximately 10 μM [5, 21]. Furthermore, the D-form of conjugated $_D(KLAKLAK)_2$ is advantageous, with significantly higher cytotoxic activity than that of the L-form and with in vivo stability that avoids degradation by blood proteases [5]. The antitumor activity of KLA has been strongly enhanced by its conjugation with cell-penetrating peptides [7, 22–25]. N-terminal and C-terminal KLA conjugation with the R7 penetrating peptide demonstrates the same cytotoxic activity [26]. Vessel-targeting peptide-modified KLA peptides, including RGD-GG-$_D$(KLAKLAK)$_2$, NGR-GG-$_D$(KLAKLAK)$_2$ [7], and RAFT-RGD-KLA [22], are especially toxic to angiogenic endothelial cells, leading to reduced tumor growth and metastases, as well as prolonged survival. However, due to the lack of penetration ability in tumor vessels, higher concentrations injected intratumorally or intraperitoneally but not intravenously limit the use of these peptides.

We coupled KLA to the N-terminus of iRGD in $_D(KLAKLAK)_2$-iRGD and $(KLAKLAK)_2$K-iRGD fusion peptides to test whether these constructs could selectively inhibit tumor cell growth in vivo. The difference between these two peptides is that the L-enantiomeric amino acid bond A_LK- has been proven to be a specific substrate of CTSB, and the effect of CTSB is decreased when using the A_DK-bond [17, 27, 28]. The A_LK-bond is selectively activated by CTSB in lysosomes (pH = 5.0) and is relatively stable in circulation

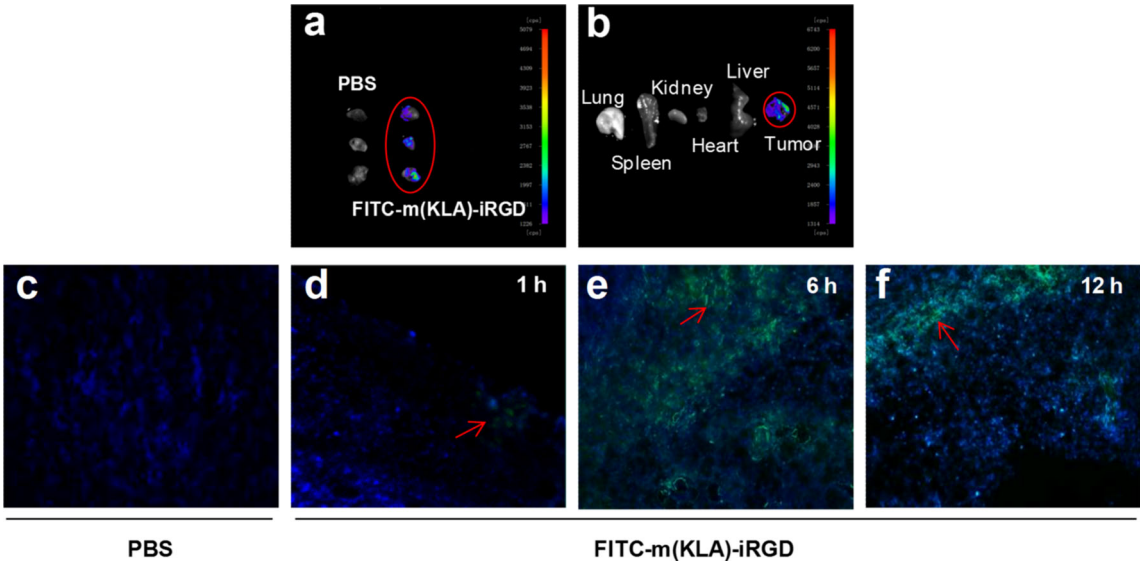

Fig. 4 Penetration of m(KLA)-iRGD into tumor tissue in vivo. **a**, **b** FITC-m(KLA)-iRGD targeting 4T1 tumors in vivo. One hundred micrograms of FITC-m(KLA)-iRGD (*green*) or PBS was intravenously injected into 4T1-bearing mice for 6 h. The mice tissues were imaged by an in vivo imaging system. Fluorescent microscopic view of 4T1 tumor explants incubated with DAPI (*blue*). Images of serial sections from 4T1 tumors injected with PBS (**c**) and m(KLA)-iRGD (**d**–**f**) for different times before harvesting the tumor

(pH = 7.0) [17]. Therefore, due to the intracellular release of nonmodified KLA, our results showed that m(KLA)-iRGD had better cytotoxicity against the tumor cell lines compared to $_{D}$(KLA)-iRGD, which cannot be digested by CTSB. This result indicates that the L-enantiomer of the N-terminal K of KLA is required for digestion, and intracellular exposure of the C-terminus of KLA can enhance the cytotoxicity of $_{D}$(KLA)-iRGD.

In addition, m(KLA)-iRGD showed distinct cytotoxic properties in different cell lines. For example, m(KLA)-iRGD played the antitumor role only in NRP1+/αvβ3+ double positive tumor cell lines, and the inhibitory effect of m(KLA)-iRGD was enhanced in CTSB+ tumor cell lines. By binding of the RGD motif to αvβ3 integrin, selective binding of the CendR motif to NRP1, and release of the KLA motif, m(KLA)-iRGD targets tumor tissues, selectively

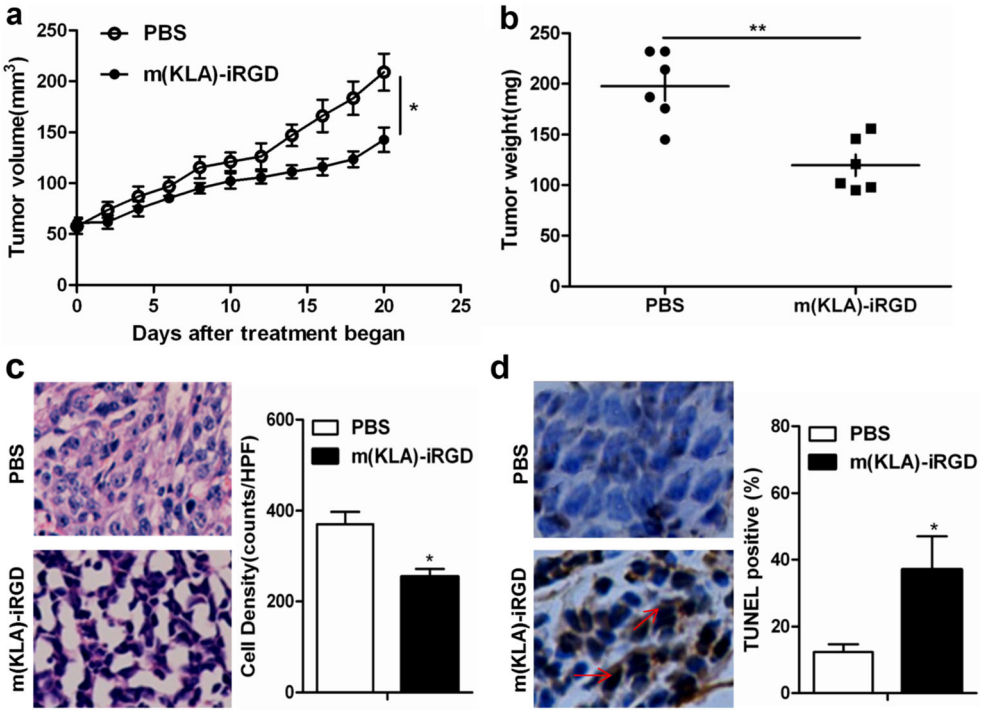

Fig. 5 Inhibitory effect of m(KLA)-iRGD on tumor growth in vivo. Mice bearing 4T1 tumors were treated by intravenous injections of PBS or m(KLA)-iRGD every other day for 3 weeks. **a** The mean tumor volume was plotted. Two-way ANOVA was used for the analysis of tumor volume and one-way ANOVA for tumor weight. *$P = 0.011$. **b** The mean weights of the tumors were measured ($P = 0.018$). **c** Tumor tissues were removed and measured at the end of the treatment. H&E staining of tumor sections from mice treated with m(KLA)-iRGD and PBS control. **d** Cell death was analyzed by TUNEL staining (*brown*). Nuclei were stained with DAPI (*blue*)

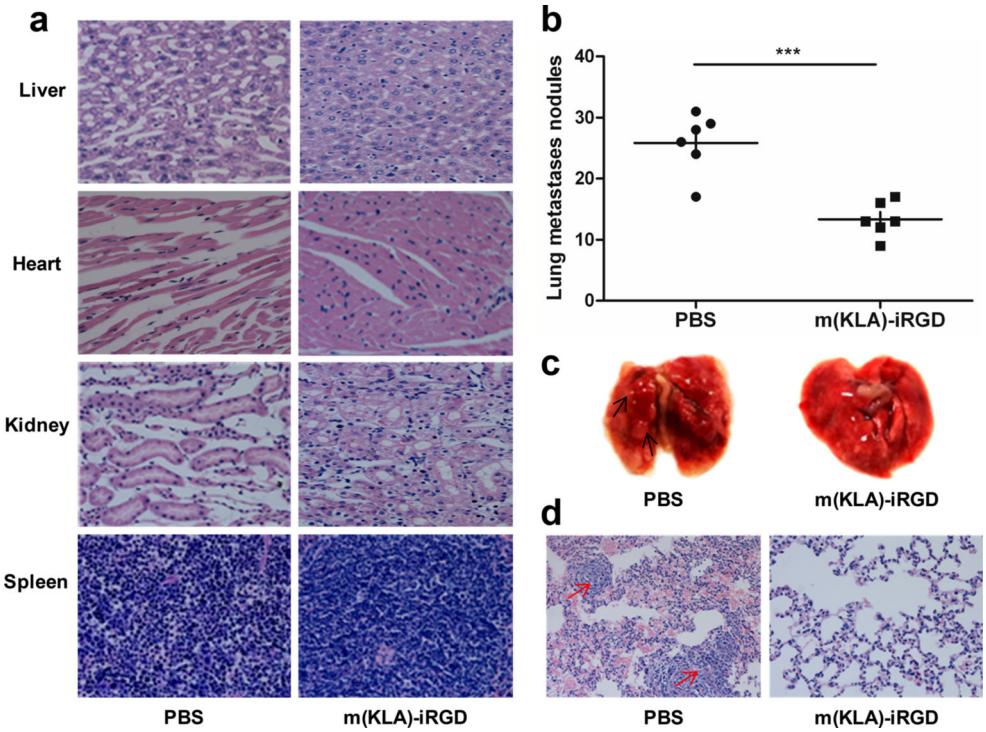

Fig. 6 Inhibitory effect of m(KLA)-iRGD on tumor metastasis in vivo. **a** H&E staining of the liver, lung, and kidney sections from mice treated with m(KLA)-iRGD and PBS control. **b**, **c** Fewer lung metastatic nodules were observed in m(KLA)-iRGD-treated mice than the PBS control. **d** H&E staining of lung sections of mice treated with PBS or m(KLA)-iRGD

killing tumor cells by activating a caspase-independent, mitochondrial cell death pathway. Targeting caspase-independent pathways for tumor therapeutics is a promising strategy to eliminate cancer cells because tumor cells often develop resistance to antitumor agents by developing defects in caspase activation [6, 29]. The dual selective properties of m(KLA)-iRGD could be an advantage, especially with fewer side effects in the single NRP1+ normal cells, enhancing the specificity of antitumor drugs. Our study showed that the cytotoxicity of m(KLA)-iRGD is significantly higher in $NRP^+/CTSB^+$ cells than in $NRP^+/CTSB^-$ tumor cells, which indicates that m(KLA)-iRGD was designed to be cytolytic to $\alpha v\beta 3+/NRP^+/CTSB^+$ tumor cells. This highly selective property may lead to a reduction in the side effects in nontumor tissues that lack CTSB overexpression.

Upon arrival at the tumor cell, m(KLA)-iRGD was digested by CTSB to release iRGD and KLA. Released iRGD can then inhibit metastasis as mediated by the CendR motif [10]. Treatment of tumor-bearing mice with m(KLA)-iRGD effectively inhibited tumor growth and metastasis in vitro, causing an approximately 30 % reduction in tumor volume of 4T1 tumors and a 40 % reduction in tumor cell density when treated at lower concentrations intravenously. Specifically, m(KLA)-iRGD effectively inhibits metastasis, and our study showed that m(KLA)-iRGD completely inhibited lung metastasis. These results are consistent with Sugahara KN's report [9] and identified the effect of this iRGD-mediated delivery system in inhibiting metastasis.

Overall, the m(KLA)-iRGD (i) effectively drives the cytolytic peptide KLA into the tumor tissues, (ii) cleaves m(KLA)-iRGD by CTSB to release the KLA and iRGD peptides inside tumor cells, and (iii) induces apoptosis of tumor cells and inhibits tumor metastasis by KLA by cooperating with iRGD. Our results show that the encapsulation of a fusion peptide containing specific targeting moieties may be useful for the systemic treatment of tumors. As a novel tumor-penetrating cytolytic peptide, m(KLA)-iRGD may be a promising candidate therapeutic agent for metastatic tumors based on its specific dual-targeting and effective tumor-inhibiting activities.

Materials and methods

Peptide design and synthesis

Two antitumor peptides, $_D$(KLAKLAKKLAKLA)-K-GG-CRGDKGPDC (m(KLA)-iRGD) and $_D$(KLAKLAK)$_2$-GG-CRGDKGPDC ($_D$(KLA)-iRGD), were designed by coupling the iRGD targeting domain and the KLA pro-apoptotic domain via a glycinylglycine bridge. Both antitumor peptides and control peptides (iRGD and $_D$(KLAKLAK)$_2$) were synthesized using Fmoc chemistry in a solid-phase synthesizer (Biotage, Isolera Dalton) and were purified by HPLC using peptides from Bio-tech Ltd. (Shanghai, China). The sequence and structure of the indicated peptides were confirmed by mass spectrometry. Peptides were dissolved in PBS to a concentration of 1 mM.

Cell culture

Mouse breast cancer cell line 4T1, melanoma tumor cell line B16, human breast cancer cell line MDA-MB-231, and SKBR3 (Chinese Academy of Sciences, Shanghai, China) were cultured in RPMI medium 1640 (Invitrogen, CA, USA) supplemented with 10 % heat-inactivated fetal bovine serum, 100 U/ml penicillin, and 10 μg/ml streptomycin at 37 °C in a 5 % CO_2 atmosphere.

Fluorescent images

Cells were seeded onto glass coverslips and cultivated for 24 h until reaching 60 % confluence. The medium was replaced with 1 ml of fresh medium supplemented with 10 % fetal bovine serum and 1 μM FITC-conjugated peptide. The cells were then cultivated for 2 h. The cells were washed with PBS three times and then were fixed with methanol/acetone (1:1). The nuclei of tumor cells were visualized using 4,6-diamidino-2-phenylindole (DAPI) staining. The cells were examined under a confocal microscope (Zeiss LSM710).

Cell viability assay

Cell viability was measured using the 3-(4,5-dimethylthiazol-2yl)-2,5-diphenyl-tetrazolium bromide (MTT, Sigma) colorimetric dye method. Briefly, 4T1, MDA-MB-231, SKBR3, and B16 cells were plated overnight at 5000 cells per well in 96-well plates. Cells were then treated with 10, 20, 30, and 40 μM of m(KLA)-iRGD and control peptides for 24 to 72 h. Three independent experiments have been performed, each performed in three replicates. The inhibition of cell growth was measured and calculated according to the following formula: inhibition rate (%) = (control value A490 − experimental value A490) / control value A490 × 100 %.

Flow cytometry

Cells that were 80 % confluent were treated with 20 μM m(KLA)-iRGD for 24 h. Cells were observed under an inverted microscope (Nikon TE 300), harvested in 5 mM EDTA in PBS, washed and resuspended in Annexin-binding buffer, and then stained with Annexin V and propidium iodide (PI) according to the manufacturer's instructions (Calbiochem, San Diego, CA). Apoptotic cells were analyzed by FACS Calibur (BD Biosciences). Experiments were conducted in triplicate.

Western blotting analysis

Total cell proteins were separated by 12 % SDS-PAGE, transferred to polyvinylidene difluoride membranes, and probed with antibodies directed against human caspase-3, cleaved caspase-3, cleaved caspase-8, cleaved caspase-9, and Bcl-2 (1:1000, Cell Signaling Technology Inc., USA), CTSB, avβ3 and NRP-1 (1:2000, Lab Vision & NEOMARKERS), and β-actin (1:5000, Santa Cruz Biotechnology). Horseradish peroxidase-conjugated goat anti-rabbit antibody was used as the secondary antibody. Proteins were visualized with chemiluminescence reagents (Santa Cruz Biotechnology).

Mouse experimental techniques

Four-week-old BALB/c female mice were obtained from the Sun Yat-sen University (Guangzhou, China) Animal Center and raised under pathogen-free conditions. All of the animal studies were conducted in accordance with institutional guidelines for the care and use of experimental animals. The mice were inoculated subcutaneously under the right shoulder with 2×10^6 4T1 cells.

For the drug treatment, 5 days after tumor transplantation, 10 mg/kg m(KLA)-iRGD peptide or PBS was injected intravenously via tail veins every other day. Tumor growth and body weight were monitored every 2 days. Tumor growth was measured in three dimensions twice a week by a caliper. Tumor volume was calculated using the following formula: length × width^2 × 0.52. The m(KLA)-iRGD peptide-treated mice were sacrificed 3 weeks after the treatment began, and the tumors were surgically removed and counted. The tissues were fixed in 10 % neutral-buffered formalin solution prepared for H&E staining or TUNEL assays.

For in vivo imaging, tumor-bearing mice with tumors sized 1.0–1.5 cm^3 were injected with FITC-conjugated peptide (100 μg in 100 μl of PBS) intravenously via the tail vein, and the peptide was allowed to circulate for the indicated time. The mice were then anesthetized and perfused with 20 ml of PBS through the left ventricle at the indicated time points. Tumors and control organs, including the heart, liver, spleen, lung, and kidney, were collected and observed using a Berthold NightOWL LB 983 Imaging System (Bad Wildbad, Germany). For fluorescence imaging, those tumors and control organs were frozen in embedding medium (Tissue-Tek, Elkhart, USA), sliced, and examined for fluorescence using fluorescence microscopy (Zeiss LSM710). The nuclei of tumor cells were visualized by DAPI staining.

Histology

Tumor tissues were fixed in 10 % buffered formalin for 24 h, processed, and embedded in paraffin for sectioning according to the conventional methods. The paraffin-embedded 4T1 tissues were sectioned into 5-μm-thick sections. The sections were dewaxed, rehydrated, and rinsed.

The tumor cell density in H&E-stained sections was calculated by scanning the tissue sections under a ×40-power microscope and counting the number of nuclei of each histological image in ten different, random fields. Data were averaged over ten fields for statistical analysis.

TUNEL staining of the tissue sections was performed using an In Situ Cell Death Detection Kit (Roche, Indianapolis, IN, USA) according to the manufacturer's instructions. The slides were counterstained with hematoxylin (blue). Tumor cell nuclei were quantified by randomly counting 10 fields/section. The apoptotic index (percentage of apoptotic nuclei) was calculated as apoptotic nuclei / total nuclei counted × 100.

Statistical analysis

All of the analyses were conducted using SPSS 16.0 (SPSS Inc., Chicago, IL, USA). The two-tailed test was used for comparisons between groups. $P < 0.05$ was defined as statistically significant. All of the values are presented as the mean ± standard deviation (SD).

Acknowledgments This work was supported by the National Natural Science Foundation of China (No. 81072670) and the Fundamental Research Funds for the Central Universities.

Compliance with ethical standards

Ethics statement All of the animal procedures and experiments were approved by the Institutional Ethical Committee for Animal Research at Sun Yat-sen University. Twelve female BABL/c mice were used in the study.

Conflicts of interest None

References

1. Hait WN. Targeted cancer therapeutics. Cancer Res. 2009;69:1263–7.
2. Minchinton AI, Tannock IF. Drug penetration in solid tumours. Nat Rev Cancer. 2006;6:583–92.
3. Svensen N, Walton JG, Bradley M. Peptides for cell-selective drug delivery. Trends Pharmacol Sci. 2012;33:186–92.
4. Chen R, Braun GB, Luo X, Sugahara KN, Teesalu T, Ruoslahti E. Application of a proapoptotic peptide to intratumorally spreading cancer therapy. Cancer Res. 2013;73:1352–61.
5. Ellerby HM, Arap W, Ellerby LM, Kain R, Andrusiak R, Del Rio G, et al. Anti-cancer activity of targeted pro-apoptotic peptides. Nat Med. 1999;5:1032–8.
6. Cieslewicz M, Tang J, Jonathan LY, Cao H, Zavaljevski M, Motoyama K, et al. Targeted delivery of proapoptotic peptides to tumor-associated macrophages improves survival. Proc Natl Acad Sci. 2013;110:15919–24.
7. Smolarczyk R, Cichoń T, Graja K, Hucz J, Sochanik A, Szala S. Antitumor effect of RGD-4C-GG-D (KLAKLAK) 2 peptide in mouse B16 (F10) melanoma model. Acta Biochim Pol. 2005;53:801–5.
8. Lemeshko VV. Potential-dependent membrane permeabilization and mitochondrial aggregation caused by anticancer polyarginine-KLA peptides. Arch Biochem Biophys. 2010;493:213–20.
9. Sugahara KN, Teesalu T, Karmali PP, Kotamraju VR, Agemy L, Greenwald DR, et al. Coadministration of a tumor-penetrating peptide enhances the efficacy of cancer drugs. Science. 2010;328:1031–5.
10. Sugahara KN, Braun GB, de Mendoza TH, Kotamraju VR, French RP, Lowy AM, et al. Tumor-penetrating iRGD peptide inhibits metastasis. Mol Cancer Ther. 2015;14:120–8.
11. Ruoslahti E, Bhatia SN, Sailor MJ. Targeting of drugs and nanoparticles to tumors. J Cell Biol. 2010;188:759–68.
12. Lao X, Liu M, Chen J, Zheng H. A tumor-penetrating peptide modification enhances the antitumor activity of thymosin alpha 1. PLoS One. 2013;8(8):e72242.
13. Yang X-Z, Du X, Wang J-W, Zhang R, Zhao J, Wang F-J, et al. Enhancing tumor-specific intracellular delivering efficiency of cell-penetrating peptide by fusion with a peptide targeting to EGFR. Amino Acids. 2015;47:997–1006.
14. D'Onofrio N, Caraglia M, Grimaldi A, Marfella R, Servillo L, Paolisso G, et al. Vascular-homing peptides for targeted drug delivery and molecular imaging: meeting the clinical challenges. Biochim Biophys Acta Rev Cancer. 2014;1846:1–12.
15. Beer AJ, Schwaiger M. Imaging of integrin αvβ3 expression. Cancer Metastasis Rev. 2008;27:631–44.
16. Jubb AM, Strickland LA, Liu SD, Mak J, Schmidt M, Koeppen H. Neuropilin-1 expression in cancer and development. J Pathol. 2012;226:50–60.
17. Dubowchik GM, Firestone RA, Padilla L, Willner D, Hofstead SJ, Mosure K, et al. Cathepsin b-labile dipeptide linkers for lysosomal release of doxorubicin from internalizing immunoconjugates: Model studies of enzymatic drug release and antigen-specific in vitro anticancer activity. Bioconjug Chem. 2002;13:855–69.
18. Sinha AA, Morgan JL, Betre K, Wilson MJ, Le C, Marks LS. Cathepsin B expression in prostate cancer of native Japanese and Japanese-American patients: an immunohistochemical study. Anticancer Res. 2008;28:2271–7.
19. Chan AT, Baba Y, Shima K, Nosho K, Chung DC, Hung KE, et al. Cathepsin B expression and survival in colon cancer: implications for molecular detection of neoplasia. Cancer Epidemiol Biomark Prev. 2010;19:2777–85.
20. Gong F, Peng X, Luo C, Shen G, Zhao C, Zou L, et al. Cathepsin b as a potential prognostic and therapeutic marker for human lung squamous cell carcinoma. Mol Cancer. 2013;12:10.1186.
21. Blondelle SE, Houghten RA. Design of model amphipathic peptides having potent antimicrobial activities. Biochemistry. 1992;31:12688–94.
22. Dufort S, Sancey L, Hurbin A, Foillard S, Boturyn D, Dumy P, et al. Targeted delivery of a proapoptotic peptide to tumors in vivo. J Drug Target. 2011;19:582–8.
23. Karjalainen K, Jaalouk DE, Bueso-Ramos CE, Zurita AJ, Kuniyasu A, Eckhardt BL, et al. Targeting neuropilin-1 in human leukemia and lymphoma. Blood. 2011;117:920–7.
24. Alves ID, Carré M, Montero MP, Castano S, Lecomte S, Marquant R, et al. A proapoptotic peptide conjugated to penetratin selectively inhibits tumor cell growth. Biochim Biophys Acta. 1838;2014:2087–98.
25. Kim HY, Kim S, Youn H, Chung JK, Dong HS, Lee K. The cell penetrating ability of the proapoptotic peptide, KLAKLAKKLAKLAK fused to the N-terminal protein

transduction domain of translationally controlled tumor protein, MIIYRDLISH. Biomaterials. 2011;32:5262–8.
26. Lemeshko VV. Electrical potentiation of the membrane permeabilization by new peptides with anticancer properties. Biochim Biophys Acta Biomembr. 2013;1828:1047–56.
27. Dubowchik GM, Mosure K, Knipe JO, Firestone RA. Cathepsin B-sensitive dipeptide prodrugs. 2. Models of anticancer drugs paclitaxel (Taxol®), mitomycin C and doxorubicin. Bioorg Med Chem Lett. 1998;8:3347–52.
28. Zhong Y-J, Shao L-H, Li Y. Cathepsin B-cleavable doxorubicin prodrugs for targeted cancer therapy (review). Int J Oncol. 2013;42:373–83.
29. Bröker LE, Kruyt FA, Giaccone G. Cell death independent of caspases: a review. Clin Cancer Res. 2005;11:3155–62.